Separation Science and Technology
Publication details, including instructions for authors and subscription information:
http://www.informaworld.com/smpp/title~content=t713708471

Application of Magnetically Stabilized Fluidized Beds for Cell Suspension Filtration from Aqueous Solutions

Z. Al-Qodah[a]; M. Al-Shannag[a]
[a] Department of Chemical Engineering, Faculty of Engineering Technology, Al-Balqa Applied University, Amman, Marka, Jordan

To cite this Article Al-Qodah, Z. and Al-Shannag, M.(2007) 'Application of Magnetically Stabilized Fluidized Beds for Cell Suspension Filtration from Aqueous Solutions', Separation Science and Technology, 42: 2, 421 — 438
To link to this Article: DOI: 10.1080/01496390600997807
URL: http://dx.doi.org/10.1080/01496390600997807

Separation Science and Technology, 42: 421–438, 2007

ISSN 0149-6395 print/1520-5754 online
DOI: 10.1080/01496390600997807

Application of Magnetically Stabilized Fluidized Beds for Cell Suspension Filtration from Aqueous Solutions

Z. Al-Qodah and M. Al-Shannag
Department of Chemical Engineering, Faculty of Engineering Technology, Al-Balqa Applied University, Marka, Amman, Jordan

Abstract: A magnetically stabilized fluidized bed (MSFBs) utilizing a transverse magnetic field was used to retain cells from cell suspension. The magnetic field permits bed expansion without mixing of the magnetic particles. The bed porosity increased by 75% when the magnetic field intensity increases to 110 mT. The effect of the magnetic field, suspension flow rate, bed height, initial concentration, and pH on the breakthrough curves was studied. According to the experimental results, increasing the initial concentration, flow rate, and pH leads to early breakthrough and inefficient deposition. Additionally, increasing the field intensity and bed height delays the breakthrough point.

Keywords: Magnetic stabilization, magnetically stabilized fluidized beds, cell suspension, magnetic field, cell filtration

INTRODUCTION

Liquid effluents of many biochemical and biomedical processes utilizing cellular materials such as whole cell fermentation processes usually contain appreciable amounts of washed out cells, cell aggregates, or cell debris. Even in the case of immobilized cell bioprocesses, significant amounts of detached cells are usually eluted from the support and appeared in the

Received 4 April 2006, Accepted 29 August 2006
Address correspondence to Z. Al-Qodah, Department of Chemical Engineering, Faculty of Engineering Technology, Al-Balqa Applied University, P.O. Box 340558, Marka, Amman 11134, Jordan. E-mail: zakaria_al_qodah@fet.edu.jo or z_alqodah@hotmail.com

reactor effluent. If the target products are soluble in these liquid effluents, then the removal of the cellular materials from these effluents is of primary concern prior to any further downstream processes required for the recovery of the products. In addition, in biomass producing processes such as single cell protein, the cells are the desired product and in some cases suitable solid-liquid separation devices must adequately dewater the cell suspension.

Currently, there are a wide variety of bioseparation techniques used in different biotechnological applications. These techniques include: centrifugation, filtration, sedimentation, flocculation, floatation, and adsorption. Among these techniques centrifugation and filtration are the most widely used bioseparation techniques. However, centrifugation is usually accompanied with heat generation and high shear forces that may damage the cells, whereas filtration using membranes suffers from a clogging problems. Furthermore, sedimentation which is a very simple technique should be coupled with the flocculation process in the case of small cells processing in order to reduce the relatively long sedimentation time.

Another versatile separation technique used to separate solid particles from liquid effluents is the packed bed usually called deep-bed filter. The solid suspensions in the liquid streams passing through these beds usually deposit throughout the entire surface of the filter media until the whole surface area of the bed granules is covered by the retained solids (1). At that moment, the bed usually suffers from high pressure drop and clogging from specific and/or nonspecific binding (2). Consequently, the bed should be regenerated by removing the collected solid particles. For ideal behavior, i.e., minimizing drawbacks while maintaining the advantages, improvement in the performance of deep-filters is needed. The above two drawbacks should be eliminated and the retention capacity of the bed could be increased by increasing the void fraction in the bed. The deep-bed filter is expected to be modified to that behavior by providing a solid-phase of magnetic particles and applying the principle of magnetic stabilization (3). The application of a magnetic field to a bed of ferromagnetic particles induces magnetic cohesive forces among the particles and tends to imposes anisotropy in their arrangement along the field lines (4–9). The passage of a liquid stream through the magnetized system transfers the bed to a more expanded state usually called magnetically stabilized fluidized bed (MSFB). The bed expansion usually increases as the liquid velocity increases until the bed height becomes as much as the magnetic system height (10).

In biotechnology, there has been a variety of separation approaches under the effect of magnetic field (11–13). However, the two-phase magnetically stabilized fluidized bed (MSFB) has recently emerged as an efficient and promising separation technique in many biochemical and biomedical applications. It has successfully been used as a filter or adsorber to separate nucleic acids, cells, cell debris, protein molecules, and antibodies from different liquid effluents (3, 13–15). In a more recent study and to allow for wider operating conditions than conventional filters, Putnam et al. (2) used

MSFBs to accomplish fractionation of *Erythrocyte* subpopulation. The above studies show that (MSFB) exhibits very desired characteristics such as high liquid throughputs, improved contact between the liquid and solid phases, elimination of bed clogging, and low pressure drop. In addition, these contactors are characterized by low shear rates due to the expanded and fluid-like structure of the bed and the ability to firmly control and retain low density magnetic particles (6, 16–18). It was found that the bed was very gentle towards highly viscous mediums such as blood or mediums containing living cells or large protein molecules. As a consequence no cell or large molecules damage takes place in the bed even at very high convective transport rates (2, 13).

Nevertheless, the orientation of the magnetic field applied in most previous studies is axial and generated from powered wire coils which surrounded the separation vessel. In addition, the resultant magnetic field from such a system could be non-homogenous and the magnetic coils temperature could increase to unsafe values if the coils are too close to the working vessel (17, 19–21). Moreover, the limited studies used transverse to the flow fields installed two permanent magnets and the magnetic field intensity was adjusted according to tedious procedures by varying the distance between the two magnets and changing the vertical position of the vessel (22). For these reasons, the primary objective of this study is to remove cells from aqueous solutions using magnetically stabilized fluidized beds employing an improved design of the magnetic system overtaking most of the above limitations.

Since cell removal mechanism in MSFBs is dominated by intra particle diffusion followed by sedimentation on the outer surface of the bed particles rather than diffusion in the pores of the particles (1), bed porosity is considered as one of the major parameters affecting the bed performance. The effect of some hydrodynamic and operational parameters affecting cell removal efficiency, η, collision efficiency, α, and breakthrough curves will be investigated in the presence of the applied magnetic field. These parameters include: bed expansion and porosity, liquid flow rate, initial bed height, pH, and inlet concentration.

MATERIAL AND METHODS

Materials

Yeast cells (*Saccharomyces cerevisiae*) were purchased from Astrico (Jordan). Double distilled water was used to prepare cell suspensions at different concentrations. Magnetic particles were prepared in the same manner as described earlier (23). The characteristics of these particles are shown in Table 1. The nonporous magnetic particles used consist of a ferromagnetic core of magnetite (Fe_3O_4) covered by a stable layer of activated carbon or zeolite by using epoxy resin as an adhesive. These particles are normally fluidized in the absence of the magnetic field and they are considered as non-porous

Table 1. Characteristics of the magnetic particles used in this study

Material used to cover magnetite	ρ_b (kg/m^3)	ρ_s (kg/m^3)	Shape factor	d_p (mm)	U_{lmfo} (m/s)	B_s (mT)	Porosity ε_o (−)
Activated carbon	1600	2760	0.9	0.7	1.05	590	0.42

particles with good adhesion properties for cells (23). The activated carbon magnetic particles have black color. This color facilitates visual observations in the hydrodynamic study.

A schematic diagram of the experimental setup is shown in Fig. 1. Column (1) was made of transparent Plexiglas with an inner diameter of 0.045 m and height H of 0.75 m. A perforated non-magnetic stainless steel grid (2) of 0.0003 m pore diameter was mounted on the base of the column to support the solid phase (3) and distribute the influent cell suspension coming from the tank (10), which is equipped with a mixer (6) via a centrifugal pump (11).

The magnetic system (13) is made of a cast steel core which consists of 180 painted cast steel sheets of 9×10^{-3} m thickness. A copper coil consisting of

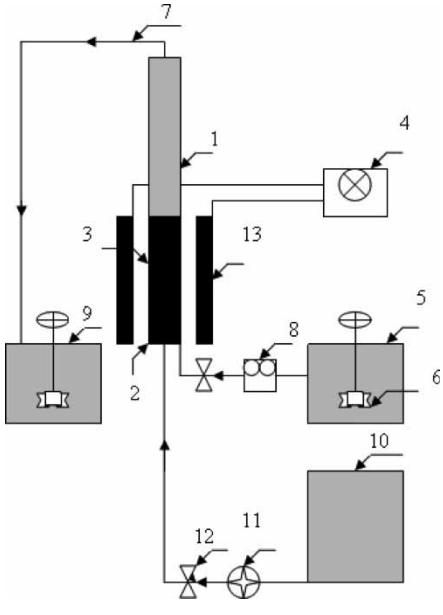

Figure 1. Schematic of the experimental apparatus. 1. Column, 2. Supporting grid, 3. Magnetic particles, 4. Power supply, 5. Feed tank, 6. Mixer, 7. Effluent stream, 8. Peristaltic pump, 9. Effluent receiver, 10. Distilled water, 11. Centrifugal pump, 12. Valve, 13. Magnetic system.

1500 turns of a copper wire of 9×10^{-3} m diameter. Glass wool was used as an insulator between the layers of the core. The shape of the cast steel sheets and the resultant shape of the magnetic core were suitable to house the column and are described elsewhere (10, 18). The net height of the magnetic system is 0.20 m and its net weight is 40 kg. The DC current was supplied from a power supply (4) can be varied from 0 to 5 Ampere and the corresponding magnetic field intensity changes from zero to 200 mT. As mentioned before, this magnetic system produces concentrated and homogeneous magnetic field as indicated by Hall probe. In addition, it minimizes electrical energy losses in the form of heat when compared to electromagnets made of solenoids only (10). The evidence of this fact was that the temperature of the magnetic system has not arisen above 35°C for one hour of continuous operation.

Methods

The cell concentration in the inlet feed to the stabilized bed and in the leaving stream was determined continuously by absorbance measurements using spectrophotometer (Philips) at a wave length of 610 nm. A calibration curve between cell concentration (ppm) and turbidity is shown in Fig. 2. The leaving stream (7) was collected in tank (9) in order to calculate the cell removal efficiency, cell loading, and the collision efficiency under the effect of a selected parameter such as initial concentration, flow rate, pH, or bed height. The removal efficiency, η, the cell loading on the magnetic particles, q, and the collision efficiency, α, (24) were calculated using the following equations:

$$\eta = (C_o - C)/C_o \tag{1}$$

$$q = \frac{V(C_o - C)}{m} \tag{2}$$

$$\alpha = -4/3\left[\frac{r_p}{1 - \varepsilon_b}\eta L\right]\ln(C/C_o) \tag{3}$$

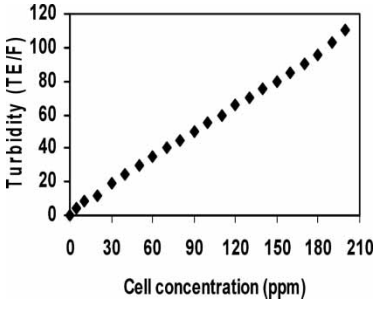

Figure 2. Calibration curve between cell concentration and turbidity.

Where C_o and C are cell concentration in the inlet feed and the collected effluent, V is the volume treated and equals to 4 liters in all experiments unless stated and m is mass of the bed (g), L is the bed height (m), ε_b is the bed porosity, r_p is the radius of the bed particles (m).

The flow regimes (bed behavior) were classified based on visual observation in the same manner as described before (6, 8, 10). The bed height was determined visually, using a ruler attached to the column wall. Liquid was pumped to the column using a peristaltic pump (GallenKamp, UK). The magnetic field intensity was measured using Hall probe (Leybolo-Heraeus, Germany).

The following equations hold for the initial solid holdup, ε_{so}, and solid holdup after bed expansion ε_s and the bed porosity, ε, respectively:

$$\varepsilon_{so} = \frac{W/\rho_s}{AH_{bo}} \tag{4}$$

$$\varepsilon_s = 1 - \frac{H_{bo}}{H_b}\varepsilon_{so} \tag{5}$$

$$\varepsilon_s = 1 - \varepsilon_s \tag{6}$$

Both ε_s and ε_b are affected by the intensity of the applied magnetic field.

Experiments in this study were conducted in the mode "Magnetizing first" (6, 19). In this mode of operation, the magnetic field was set at the desired value and applied to the packed bed. After that distilled water was fed to the column in order to transfer the bed from the initial packed to the stabilized expanded state. The water flow rate was increased until the strings of the bed start to fluidize. Then the water flow rate was gradually reduced until it was finally turned off. Then the liquid cell suspension was started with the desired flow rate. The run continued until the exit cell suspension reaches a constant value. At that point, the cell solution and magnetic field were switched off and high distilled water flow rate was started to empty the column from the cell loaded particles in order to regenerate them according to the procedure of Terranova and Burns (3). In this mode of operation and before carrying out each experiment, the bed was fluidized with distilled water in the absence of the magnetic field for 5 minutes in order to expel possible gas bubbles, followed by gradual decrease of the water flow rate until it diminishes and the bed returns to its initial packed state.

RESULTS AND DISCUSSION

Hydrodynamics of Two-Phase MSFBs

Phase Diagram

In magnetizing the first mode, the phase diagram of MSFBs usually consists of three subsequent flow regimes. These are: the initial packed bed, the stable

expanded bed, and the fluidized bed, respectively. These regimes correspond to the case where the applied magnetic field intensity is more than 10 mT to induce sufficient cohesion forces between the magnetic particles. Figure 3 shows an experimentally determined phase diagram for the magnetic particles of $U_{lmfo} = 0.009$ m/s. It can be seen from Fig. 3 that the bed exists in the initial packed bed regime if U_l is less than what is called the minimum expansion velocity, U_e. When U_l becomes greater than U_e the bed starts to expand. U_e remains constant and equal to 0.009 m/s at all values of the magnetic field. Beyond U_e, the bed begins to stably expand but without particle movement. This uniform expansion continues until the liquid velocity exceeds a second transition velocity named the minimum fluidization velocity, U_{mf} (the upper curve of Fig. 3). The magnetized system operating at $U_e < U_l < U_{mf}$ is magnetically stabilized (4–8, 10). The bed in this regime expands as U_l increases in a piston like slow and regular expansion. Furthermore, arrangement of the particle strings or chains along the field lines can be clearly observed in this regime. In addition, only *in situ* vibrations of the strings (chains-of-particles) were observed in the stabilized regime. The bed properties in these three phases are summarized in Table 2.

With further increase of U_l, the bed breaks down at the minimum fluidization velocity, U_{mf}. Above this transition velocity, the bed exists in the fluidized regime. In this regime, the fluidized system consists of strings (Chains-of-particles). It can be seen from Fig. 3 that U_{mf} increases as the applied field increases. For instance, U_{mf} increases from 0.009 to 0.042 m/s as the magnetic field intensity increases from 0 to 113 mT. The correlation between U_{mf} and B is shown in the following relation:

$$U_{mf} = U_{mfo}e^{0.0003B} \tag{7}$$

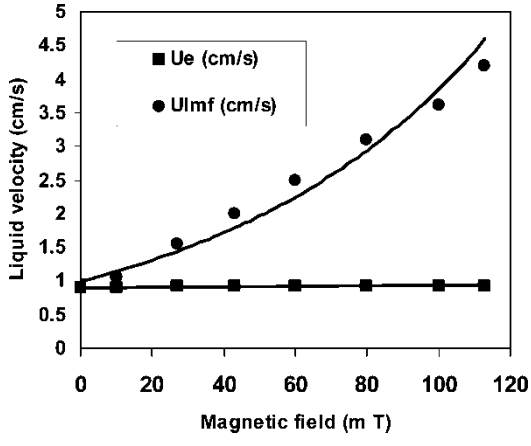

Figure 3. Phase diagram of two-phase liquid-solid magnetically stabilized fluidized beds.

Table 2. The main properties of MSFBs and the flow regimes in magnetizing first mode

Regime	Property				
	Ranges of gas velocities	Bed state	Pressure drop	Bed height	Solid mixing
Packed bed	$0 \leq U_l < U_e$	Randomly packed	High	Constant	None
Stabilized bed	$U_e \leq U_l < U_{mfo}$	Expanded with horizontal strings	Low	Increases as U_l increases	None but the bed is flowable
Fluidized bed	$U_{mf} \leq U_l < U_{pt}$	Strings then particulate fluidization	Low	Increases as U_l increases	Slow then intensive

Where B is the magnetic field intensity (mT). This equation covers B values from 0 to 113 mT and $R^2 = 0.91$.

As mentioned above, the magnetically stabilized regime bounded between U_e and U_{mf} is preferred for process operation owing to its desired properties mentioned above. For this reason, cell removal from the solution will be conducted in this regime.

Bed Expansion

Bed expansion is an important property of a fluidized system. It affects the size of the fluid-bed equipment and residence time of the liquid phase in the contactor. Figure 4 shows the bed porosity as a function of liquid velocity at different magnetic field intensities. It can be seen from Fig. 4 that an initial expansion occurs to the packed bed after the application of the magnetic field and in the absence of liquid flow as previously reported (8, 10, 19). Then beyond U_e, the bed regularly expands. The bed porosity at the onset of fluidization is the maximum porosity i.e. ε_{max} that the stabilized bed can attain.

It should be noted that a significant part of the particles surface is flat and the contact area between them in the packed regime is relatively high. This suggests that the effective surface area of the particles available for cell deposition or sedimentation is quite smaller than the total surface area of the particles. On the contrary, the bed in the stabilized regime is expanded and consists of horizontal layers of strings (6, 9, 10, 25). As a result of this new arrangement of particles, ε_{max} exceeds 0.7 as Fig. 4 indicates. This means that the bed height is almost doubled and the particles are just touching each other. Consequently, the effective outer surface area of the particles is improved and more cell deposition is expected in this regime.

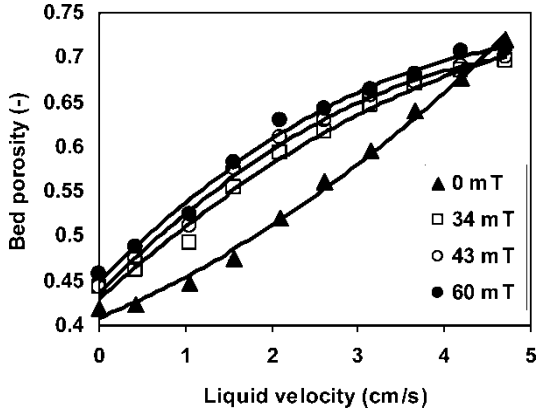

Figure 4. Effect of liquid velocity on the bed porosity at different magnetic field intensities.

There are two additional hydrodynamic parameters characterized by magnetic stabilized beds. The first parameter is the maximum porosity (ε_{max}) attained by the stabilized bed before the fluidization point which indicated the stability of the stabilized under the effect of the magnetic field and the liquid flow. The second parameter is the remaining expansion (R_{exp}) in the magnetized bed after shutting off the liquid flow through the bed which is an indication of the magnetic properties of the bed particles. Figure 5 shows the variation ε_{max} and R_{exp} as a function of the magnetic field intensity. It can be seen that for $U_l = 2.1$ cm/s, ε_{max} increases from 0.52 to 0.68 as the magnetic field intensity increases from 0 to 113 mT, respectively. Based on the data shown in Fig. 5, the following correlation

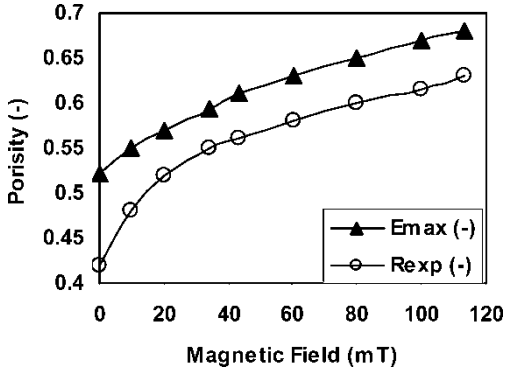

Figure 5. Effect of the magnetic field intensity on the maximum bed expansion and the remaining expansion.

relates the maximum porosity of the bed (ε_{max}) to the magnetic field intensity:

$$\frac{\varepsilon_{max}}{\varepsilon_{bo}} = -2 \times 10^{-5}B^2 + 0.0053B + 1.216 \quad (8)$$

Where ε_{bo} is the initial bed porosity. Note that in the above correlation, the values of the magnetic field intensity range from 0 to 113 mT and the value of correlation coefficient, $R^2 = 0.997$.

When U_l was gradually reduced while keeping the applied magnetic intensity constant, the bed contracts and shows hysteresis. Even when the fluid throughputs were shut off, the new reformed packed bed remained in a more expanded state than at the beginning of the experiment because the lines of magnetic field have the ability to hold the magnetic strings in an expanded state.

Figure 6 shows the bed expansion hysteresis, at two magnetic field values. It is clear from Fig. 6 that the remaining expansion at 34 and 60 mT were about 38 and 52% of the initial bed porosity ($\varepsilon_o = 0.42$). This residual expansion is eliminated and the bed returned to its original packed state when the magnetic field was shut off.

Cell Removal in MSFBs

The prediction of column breakthrough is considered as the most important criterion in the design of filters or an adsorber. The effect of some operational parameters on the breakthrough curves on MSFB particles was studied. The experiments were performed by continuous feeding of the cell suspension

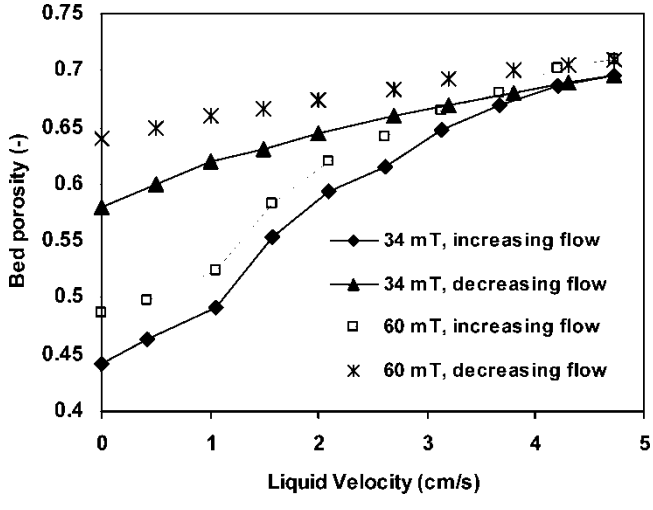

Figure 6. Bed expansion hysteresis at two magnetic field intensities.

to the bed and varying one of the operational parameters while keeping the others constant.

Effect of Magnetic Field Intensity

As shown above, one of the important consequences of the application of a magnetic field to a bed of magnetic particles is the increased bed height or porosity. This increase mainly depends on the intensity of the applied magnetic field, B, and the liquid flow rate (see Fig. 4). This implies that under the effect of these two parameters, the bed employed for filtration simultaneously manifested itself macroscopically by the overall bed expansion (10, 19). Figure 7 shows a plot of the normalized cell concentration against the volume treated, V_t at different magnetic field intensities. It can be seen from Fig. 7 that C/C_o variation with the V_t is not identical in the cases of packed ($B = 0$) and stabilized bed ($B > 0$). For instance, the values of C/C_o after treating 4 liters of the cell solution were 0.98, 0.83, 0.77, and 0.71 when B values were 0, 34, 60, and 80 mT, respectively. This means that cell deposition increases by 27% as B increases from 0 to 80 mT. These results can be understood by considering the bed porosity at these B values, which are 0.42, 0.55, 0.58, and 0.60, respectively. Since the cell solution flow rate was held constant at 40 ml/min in this part of the experiment, this implies that the interstitial liquid velocity decreases and the residence time increases as B increases. As a consequence, the liquid turbulence decreases whereas the cell deposition rate increases. Another reason for the enhancement of cell deposition in the MSFBs is related to the contact area between the bed particles. It is expected that as the bed

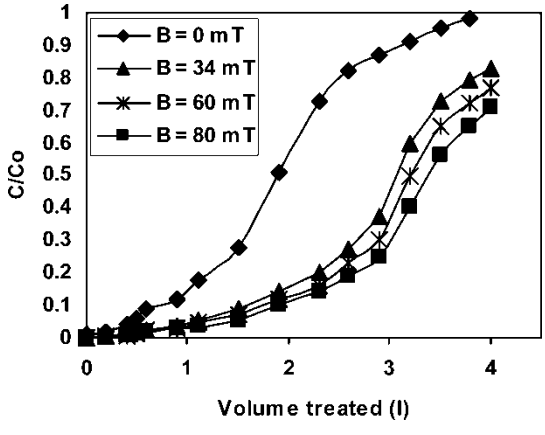

Figure 7. Variation of the normalized exit cell concentration with the volume treated at various magnetic field intensities, initial bed height = 10 cm, flow rate = 40 ml/min, pH = 7, cell concentration = 200 mg/l.

expands, the contact area between the bed particles decreases and the overall projected area for cell deposition increases. Accordingly, cell deposition becomes more efficient and easier as the bed porosity increases taking into account the absence of channels or preferential paths for liquid flow. These results are in agreement with those of Kevin et al. (15) who found the efficiency of solute removal by adsorption in magnetically stabilized bed increased significantly in the stabilized regime.

The effect of magnetic field intensity on η, q, and α is shown in Table 3. Table 3 reveals that the removal efficiency, η, the cell loading, q and the collision efficiency, α increase by 31.5, 26.8, and 282%, respectively as B increases from 0 to 80 mT. The reason for this behavior is as before, being attributed to the effect of the magnetic field on the bed porosity and consequently on the interstitial liquid velocity or the residence time. The large increase in the collision efficiency α is referred to nature of equation (3) used to evaluate it. All the parameters L, $(1/1 - \varepsilon_b)$, η and $(-\ln C/C_o)$ are strongly affected and increased as B increases.

Effect of Flow Rate

The breakthrough curves at different cell suspension flow rates are shown in Fig. 8. It is evident from Fig. 8 that cell deposition decreases as the flow

Table 3. Effect of operational parameters on the removal efficiency η, particle cell loading q, and collision efficiency α

Variable	Value	η	q (mg/g)	α ($\times 10^5$)
Magnetic field mT	0	0.49	1.6	5.625
	34	0.585	1.84	13.75
	60	0.615	1.94	18.6
	80	0.645	2.03	21.52
Flow rate ml/min	10	0.64	2.01	17.48
	20	0.61	1.93	15.36
	40	0.585	1.84	13.75
Bed height cm	6	0.5	1.57	4.55
	8	0.53	1.67	8.56
	10	0.585	1.84	13.75
	12	0.645	2.02	16.43
Initial conc. mg/l	100	0.815	1.28	36.77
	150	0.65	1.53	18.24
	200	0.585	1.84	13.35
	250	0.525	2.07	10.75
pH	5	0.59	1.86	14.06
	7	0.585	1.84	11.51
	9	0.515	1.62	9.96

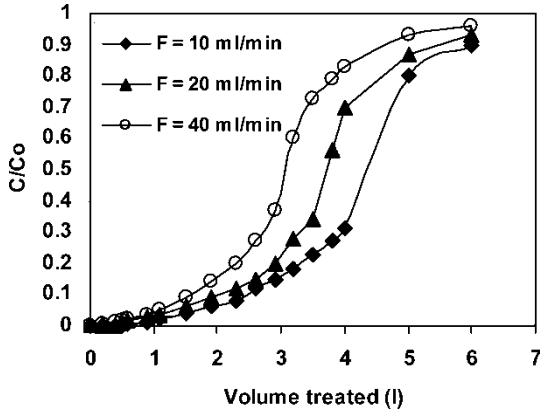

Figure 8. Variation of the normalized exit cell concentration with the volume treated at various liquid flow rates, initial bed height = 10 cm, pH = 7, cell concentration = 200 mg/l, magnetic field intensity = 34 mT.

rates increase. The volume treated, V_t corresponding to a breakthrough point of 20% i.e., $C/C_o = 0.2$ appears earlier as the flow rate increases. For example, the values of V_t are 3.4, 2.9, and 2.3 liter when the flow rate values are 10, 20, and 40 ml/min, respectively. This behavior is expected and could be attributed to the effect of the flow rate on the contact time or the interstitial liquid velocity. At constant bed height, the contact or residence time decreases and the interstitial velocity increases as the flow or dilution rate increases. As a consequence, cell deposition on the particles decreases and a postponement of the breakthrough points occurs as the flow rate increases. These results are in agreement with those of Kevin et al. (15) for the case of protein adsorption in MSFBs and those of Tong and Sun (22) who reported that the adsorption of lysozome in a magnetically stabilized bed is much better than that in packed or expanded beds. In addition, Odabasi et al. (13) reported a similar effect of liquid flow rates on the removal of antibody in a magnetically stabilized bed. Table 3 shows the values of η, q, and α corresponding to the three flow rates values. It is evident that η, q, and α increase 9.4, 9.2, and 21.0% as the flow rate decreases from 40 to 10 ml/min. The range of the changes in η, q, and α caused by the change in the flow rate is relatively small compared to that caused by the magnetic field variation. This is expected since changing the flow rate will affect the interstitial velocity in the bed only while both bed height and porosity are unchanged.

Effect of Bed Height

Figure 9 reveals the variation of the normalized effluent concentration with the volume treated at four different initial bed heights. It is evident from

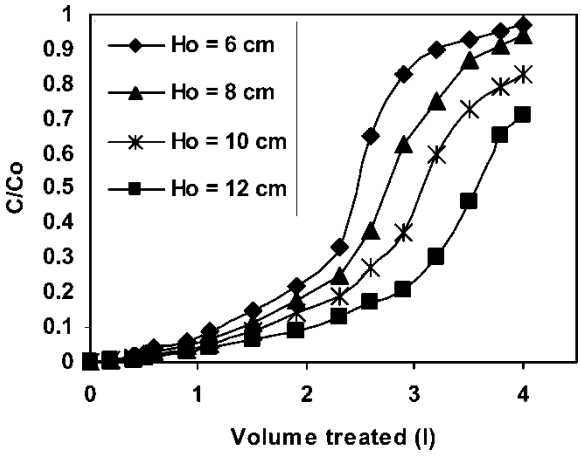

Figure 9. Variation of the normalized exit cell concentration with the volume treated at various bed heights, magnetic field intensity = 34 mT, flow rate = 40 ml/min, pH = 7, cell concentration = 200 mg/l, magnetic field intensity = 34 mT.

Fig. 9 that C/C_o in a bed of 6 cm initial height reaches 0.97 at a volume treated of 4 liters, whereas in the bed of 12 cm initial height it is only 0.71. In addition the 20% breakthrough point appears earlier in short beds. For instance, the volume treated corresponding to 20% breakthrough point for beds of 6, 8, 10, and 12 cm initial heights are 1.7, 2.05, 2.4, and 2.8, respectively. This behavior is expected because when the initial bed height decreases this implies decreasing the contact time and also decreasing the cell deposition sites in the bed forcing the cells to leave the bed at relatively shorter contact time. This fact suggests that the deposition of cells requires beds of large aspect ratio (height/diameter) in order to increase the contact time in the bed. These results are in agreement with those of Kevin et al. (15) for the case of adsorption of protein adsorption in MSFB and those of Ding and Sun (26) who reported that as the bed height increases its adsorption efficiency increases.

Table 3 shows the values of η, q, and α in these four beds. Table 3 depicts that η, q, and α increase as the bed height increases. The values of these variables increase by 29, 10, and 202% as the bed height increases from 6 to 12 cm. There is an important remark regarding the enhancement of the cell loading, q on the magnetic particles as the initial bed height increases. It was found to increase 10% when the bed height was doubled. This means that increasing the bed height will increase the overall bed loading in addition to the specific cell loading, q. This behavior could be attributed to the fact that as the bed height increases the friction between the cells and the bed particles increases to the extent that the interaction between them dominates and forces cell deposition.

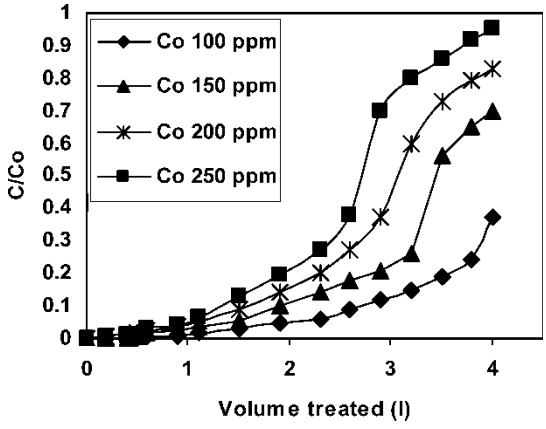

Figure 10. Variation of the normalized exit cell concentration with the volume treated at various initial cell concentrations, magnetic field intensity = 34 mT, initial bed height = 10 cm, flow rate = 40 ml/min, pH = 7.

Effect of Initial Cell Concentration

Figure 10 shows the effect of initial cell concentration on the breakthrough curves. Four different initial cell concentrations of 100, 150, 200, and 250 mg/l were used at the same flow rate of 40 ml/min and a bed of 10 cm initial height. As presented in this figure, the slope of the breakthrough curve increases as the concentration increases. As a consequence, the breakthrough point is earlier at higher concentrations. The 20% breakthrough point for the above four concentrations was reached when the volume treated values were 3.6, 2.8, 2.3, and 1.9 liters, respectively. The effect of C_o on the values of η, q, and α is shown in Table 3. It is clear that as the concentration increases from 100 to 250 mg/lη decreases by 35.6%, q increases by 61.7%, and α decreases by 70.8%. These values are reasonable since the exit normalized concentration C/C_o is strongly affected by the initial concentration as presented in Fig. 10. C/C_o values, when the volume treated is 4 liters, are 0.37 and 0.95 corresponding to C_o values of 100 and 250 mg/l, respectively. The decrease in the removal efficiency at high concentrations could be referred to the hindrance effect which reduces cell deposition. On the other hand, q increases by 61.7% because C_o increases while the bed mass does not change.

Effect of pH

The deposition of the cells from the liquid phase on the magnetic particle surface depends on the interaction between these cells and the activated carbon covering the magnetic cores. This interaction and accordingly the

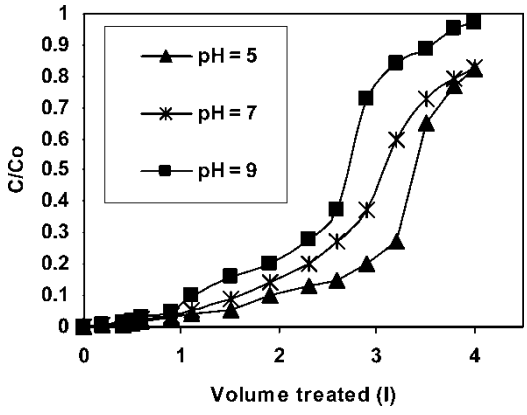

Figure 11. Variation of the normalized exit cell concentration with the volume treated at various pH, magnetic field intensity = 34 mT initial bed height = 10 cm, flow rate = 40 ml/min, cell concentration = 200 mg/l.

deposition are expected to vary according to the value of the solution pH. Figure 11 shows the variation of the normalized cell concentration with the treated volume of three solutions of three different pHs. It is clearly shown in Fig. 11 that as the pH increases the normalized concentration at the exit increases for the same treated volume. For pH values of 5, 7, and 9 the 20% breakthrough point is 2.9, 2.3, and 1.9 liters, respectively. This suggests that the interaction between the cells and the magnetic particles and consequently the deposition is enhanced by lowering the pH value of the cell suspension. It was estimated that as the pH increased from 5 to 9, the values of η, q, and α decrease by 12.7, 12.9, and 29.2% respectively. These values indicate that the collision efficiency was most affected by increasing the solution pH.

CONCLUSIONS

In this study, the application of a transverse magnetic field to a bed of magnetic particles was investigated. The resulting magnetically stabilized bed was used to remove yeast cells from cell suspension. The effect of the magnetic field on some hydrodynamic parameters affecting the cell deposition process such as bed expansion and remaining expansion was studied. The following conclusions can be drawn:

1. The bed porosity and remaining expansion increase as the magnetic field increases. This implies that at constant flow rate the interstitial velocity decreases and the contact time between the cell solution and bed particles increases.

2. The results indicate that the deposition breakthrough curve was strongly affected by the magnetic field intensity and the other studied variables such as bed height, cell concentration flow rate and pH.
3. According to the results, increasing the magnetic field and bed height leads to an early breakthrough curves and enhances the removal efficiency.
4. Increasing the initial concentration, flow rate, and pH delays the breakthrough point and reduces the removal efficiency.

REFERENCES

1. Putnam, D. and Burns, M.A. (1997) Predicting the filtration of noncoagulating particles in depth filters. *Chem. Eng. Sci.*, 52: 93.
2. Putnam, D., Namasivayam, V., and Burns, M.A. (2003) Cell affinity separations using magnetically stabilized fluidized beds, erythrocyte subpopulation fractionation utilizing a lectin-magnetite support. *Biotechnol. Bioeng.*, 81: 650.
3. Terranova, B.E. and Burns, M.A. (1991) Continuous cell suspension processing using magnetically stabilized fluidized beds. *Biotechnol. Bioeng.*, 37: 110.
4. Kirko, I.M. and Filippov, M.V. (1960) Standard correlations for a fluidized bed of ferromagnetic particles in a magnetic field. *Zn Tekhniko Fizika.*, 30: 1081.
5. Rosensweig, R.E. (1979) Fluidization: hydrodynamic stabilization with a magnetic field. *Science*, 204: 57.
6. Seigell, J.H. (1987) Liquid fluidized magnetically stabilized beds. *Powder Technol.*, 52: 139.
7. Lee, S.L.P. and Lasa, H. (1988) Radial dispersion model for bubble phenomenon in three phase fluidized beds. *Chem. Eng. Sci.*, 43: 2445.
8. Penchev, I.P. and Hristov, J.Y. (1990) Fluidization of ferromagnetic particles in a transverse magnetic field. *Powder Technol.*, 62: 1.
9. Hristov, J.H. (1996) Fluidization of ferromagnetic a magnetic field. Part 1: The effect of fields lines on the bed stability. *Powder Technol.*, 87: 59.
10. Al-Qodah, Z. (2000) Hydrodynamic behavior of a magneto airlift column in a transverse magnetic field. *Can. J. Chem. Eng.*, 78: 458.
11. Safarik, I. and Safarikova, M. (1999) Use of magnetic techniques for the isolation of cells. *Journal of Chromatography B.*, 722: 33.
12. Safarik, I. and Safarikova, M. (2004) Magnetic techniques for the isolation and purification of proteins and peptides. *BioMagnetic Research and Technol.*, 2: 1.
13. Odabasi, M., Ozkayar, N., Ozkara, S., Unal, S., and Denizli, A. (2005) Pathogenic antibody removal using magnetically stabilized fluidized bed. *Journal of Chromatography B*, 826: 507.
14. Hultman, T., Stal, S., Hornes, E., and Uhlen, M. (1989) Direct phase sequencing of genomic and plasmid DNA using magnetic beads as solid support. *Nucleic Acid Research*, 17: 4937.
15. Kevin, D., Seibert, K.D., and Burns, M.A. (1998) Effect of hydrodynamic and magnetic stabilization on fluidized bed adsorption. *Biotechnol. Prog.*, 14: 749.
16. Hristov, J.H. and Ivanova, V.N. (1999) Magnetic field assisted bioreactors. In *Recent Research Development in Fermentation and Bio-Engineering 2*; SignPost Research: Trvadrum, India; 41.
17. Zhang, Z.H., O'Sullivan, D.A., and Lyddiatt, A. (1999) Magnetically stabilized fluidized bed adsorption. Practical benefit of uncoupling bed expansion from

liquid velocities in the purification of a recombinant protein from *Escherichia coli*. *J. Chem. Technol. Biotechnol.*, 74: 270.
18. Al-Qodah, Z. and Al-Hassan, M. (2000) Phase holdup and gas-to-liquid mass transfer coefficient in magnet stabilized G-L-S airlift fermenter. *Chem. Eng. J.*, 79: 41.
19. Hristov, J.H. (2002) Magnetic field assisted fluidization—A unified approach. Part 1. Fundamentals and relevant hydrodynamics. *Reviews in Chemical Engineering*, 18: 295.
20. Hristov, J.H. (2005) External loop airlift with magnetically controlled liquid circulation. *Powder Technol.*, 149: 180.
21. Hristov, J.H. (2005) External-loop airlift magnetically stabilized bed-minimum stabilization and fluidization conditions. *China Particulogy*, 3: 197.
22. Tong, X.D. and Sun, Y. (2003) Application of magnetic agarose in liquid magnetically stabilized fluidized bed for protein adsorption. *Biotechnol. Prog.*, 19: 1721.
23. Al-Qodah, Z., Ivanova, V., Dobreva, E., Penchev, I., Hristov, J., and Petrov, R. (1991) Non-porous magnetic support for cell immobilization. *J. Ferment. Bioeng.*, 71: 114.
24. Deshpande, P.A. and Shonnnard, D.R. (2000) An improved spectrophotometric methods to study the transport, attachment, and breakthrough of bacteria through porous media. *Applied and Environmental Microbiol.*, 66: 763.
25. Hristov, J.H. (1999) Comments on gas fluidized magnetizable beds in a magnetic field, part 2: Magnetization last mode and relevant phenomena. *Thermal Science*, 2: 15.
26. Ding, Y. and Sun, Y. (2005) Small-sized dense magnetic pellicular support for magnetically stabilized fluidized bed adsorption. *Chem. Eng. Sci.*, 60: 917.